

complex adopts a "slipped-stacked" structure, similar to that of $\text{Rh}_2(\text{CNC}_6\text{H}_4\text{-}p\text{-F})_8^{2+}$,²³ with a 67° angle between the Rh-Rh vector and the $\text{Rh}(\text{CN})_4$ planes.

In the d^7 and mixed-valence systems $\text{Co}_2(\text{CNCH}_3)_{10}^{4+}$,¹⁷ $\text{Ru}(\text{CNXyl})_{10}^{2+}$,^{21b} $\text{Rh}_2(\text{CNC}_6\text{H}_4\text{-}p\text{-CH}_3)_8\text{I}_2^{2+}$,²⁵ and $\text{Rh}_3(\text{CNCH}_2\text{Ph})_{12}\text{I}_2^{3+}$,²⁶ the structures are somewhat more regular than those of the d^8 species. However, substantial variations exist even among these oxidized complexes.

Another bridged structure in the literature sheds light on the strength of the electronic forces between the metal atoms in these complexes. In $\text{Rh}_2(\text{DMB})_4^{2+}$,²⁷ the large rigid ligands are able to force the metal atoms much farther apart than they are in the other bridged and unbridged d^8 complexes. In this case, therefore, the steric constraints due to the DMB ligand appear to have overwhelmed any electronic preference for a particular Rh-Rh distance or torsion angle ω .

Summary

The crystal structures of two new d^7 - d^7 systems involving the bridging ligand TMB, including the first structure reported for a binuclear Ir(II) isocyanide complex, have been determined and compared with those of other polynuclear isocyanide complexes. Data from NMR experiments show that TMB complexes have substantial conformational mobility; this mobility may be responsible for the unusually rapid deactivation of the $^3A_{2u}$ excited state in $\text{Rh}_2(\text{TMB})_4^{2+}$.

- (25) Olmstead, M. M.; Balch, A. L. *J. Organomet. Chem.* **1978**, *148*, C15-C18. We thank Professor Balch for providing us with the atomic coordinates for this structure and the structure in ref 26.
 (26) Balch, A. L.; Olmstead, M. M. *J. Am. Chem. Soc.* **1979**, *101*, 3128.
 (27) Mann, K. R. *Cryst. Struct. Commun.* **1981**, *10*, 451.

Detailed crystallographic comparisons suggest that the bridging ligands enforce a geometrical regularity not present in the unbridged structures. The following conclusions can be drawn. While the relatively compact "bridge" ligand suffers less distortion in its Rh(II) complex than in the Rh(I) complex, the opposite is true of TMB. Torsion angles ω tend to be larger in Rh(II) and Ir(II) structures than in those of Rh(I). Also, the wide variety among the unbridged structures suggests that packing forces, either among the ligands or between the ligands and counterions, can easily surpass the electronic forces associated with bending bonds to the metal atom. Thus, the geometric preferences of the metal atoms appear to be limited to the bond length, and the steric requirements of the ligands (perhaps including the crystal packing, in the case of nonbridging ligands) appear to control the angle ω .

Acknowledgment. We thank Professor Jack D. Dunitz for making his diffractometer available for data collection on $[\text{Rh}_2(\text{TMB})_4\text{Cl}_2](\text{PF}_6)_2$. We thank Professor Dunitz, Paul Seiler, and Dr. Richard E. Marsh for numerous helpful discussions. Johnson Matthey Inc. is acknowledged for a generous loan of rhodium and iridium compounds. This research was supported by the National Science Foundation.

Registry No. $[\text{Ir}_2(\text{TMB})_4](\text{BPh}_4)_2$, 110904-71-7; $[\text{Ir}_2(\text{TMB})_4\text{I}_2](\text{BPh}_4)_2$, 99327-03-4; $[\text{Ir}_2(\text{TMB})_4\text{I}_2](\text{BPh}_4)_2 \cdot x(\text{CH}_3)_2\text{CO}$, 110904-69-3; $[\text{Rh}_2(\text{TMB})_4](\text{BPh}_4)_2$, 110904-67-1; $[\text{Rh}_2(\text{TMB})_4\text{Br}_2](\text{BPh}_4)_2$, 99326-95-1; $[\text{Rh}_2(\text{TMB})_4\text{Cl}_2](\text{PF}_6)_2$, 99326-92-8; Rh, 7440-16-6; Ir, 7439-88-5.

Supplementary Material Available: Fully labeled ORTEP^{8d} drawings for $\text{Rh}_2(\text{TMB})_4\text{Cl}_2^{2+}$ and $\text{Ir}_2(\text{TMB})_4\text{I}_2^{2+}$ and tables of positional and displacement parameters, bond distances, bond angles, and torsion angles (12 pages); tables of observed and calculated structure factors (21 pages). Ordering information is given on any current masthead page.

Contribution from the Department of Chemistry,
 University of New Mexico, Albuquerque, New Mexico 87131

Reactions of Tris(trimethylsilyl)aluminum and Ammonia. Formation, Structure, and Thermal Decomposition of $[(\text{Me}_3\text{Si})_2\text{AlNH}_2]_2$

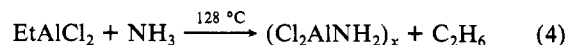
J. F. Janik, E. N. Duesler, and R. T. Paine*

Received June 25, 1987

The reaction of $(\text{Me}_3\text{Si})_3\text{Al}\cdot\text{Et}_2\text{O}$ and NH_3 in a 1:1 ratio results in the formation of $[(\text{Me}_3\text{Si})_2\text{AlNH}_2]_2$. The compound has been characterized by elemental analysis, mass, infrared, and NMR spectroscopic data, and single-crystal X-ray diffraction analysis. The compound crystallizes in the monoclinic space group $P2_1/n$ with $a = 9.364$ (1) Å, $b = 8.171$ (2) Å, $c = 16.781$ (3) Å, $\beta = 95.78$ (1)°, $Z = 2$, $V = 1277.4$ (4) Å³, and $\rho = 0.98$ g cm⁻³. Least-squares refinement gave $R_F = 4.15\%$ and $R_{wF} = 3.85\%$ on 2068 independent reflections with $F \geq 4\sigma(F)$. The molecule contains a central planar four-membered Al-N-Al'-N' ring with $\text{Al}(1)\text{-N}(1) = 1.953$ (2) Å, $\text{Al}(1)\text{-N}(1') = 1.956$ (2) Å, $\text{Al}(1)\text{-N}(1)\text{-Al}(1') = 93.1$ (1)°, and $\text{N}(1)\text{-Al}(1)\text{-N}(1') = 86.9$ (1)°. Thermolysis of the dimer or a polymeric product, obtained from reactions of $(\text{Me}_3\text{Si})_3\text{Al}\cdot\text{Et}_2\text{O}$ and excess ammonia, gives solid solutions of AlN and SiC.

Introduction

The coordination chemistry for alanes and tertiary amines has been extensively studied, and a large number of simple, stable acid-base complexes, $\text{X}_3\text{Al}\cdot\text{NR}_3$, have been isolated.¹ Alanes and NH_3 , primary amines, and secondary amines also form a large number of adducts; however, these combinations show a pronounced tendency to undergo elimination-condensation reactions, which produce amino- and imino-substituted alanes.¹ The elimination reactions appear to be dependent upon aluminum-substituent group bond strengths, showing increasing ease of elimination from the aluminum fragment in the following order: $\text{Al-Cl} < \text{Al-R} < \text{Al-H}$.¹ Reaction temperatures in the combinations shown in eq 1-4 provide qualitative evidence for part of this



series.¹⁻³ Although kinetic studies for these reaction systems are limited, it has been suggested that the elimination process is not preceded by, but instead may compete with, adduct formation. In fact, formation of an adduct may result in a "dead-end" state for elimination reactions.⁴

(1) Mole, T.; Jeffery, E. A. *Organoaluminum Chemistry*; Elsevier: New York, 1972.

(2) Cohen, M.; Gilbert, J. K.; Smith, J. D. *J. Chem. Soc.* **1965**, 1092.

(3) Gilbert, J. K.; Smith, J. D. *J. Chem. Soc. A* **1968**, 233.

(4) Beachley, O. T.; Tessier-Youngs, C. *Inorg. Chem.* **1979**, *18*, 3188.

Interest in elimination processes involving alanes and amines has been rekindled recently by efforts to find new molecular precursors for AlN.⁵ This material has been typically prepared by high-temperature direct reaction of aluminum with NH₃ or N₂⁶ or by carbothermal reduction of alumina.⁷ More recently, aluminum nitride has also been made by vapor deposition techniques on various substrates with gas mixtures containing, for example, AlCl₃ and NH₃⁸ or Me₃Al and NH₃.⁹ The majority of this chemistry is not well understood. In an effort to better understand alane-amine elimination chemistry, Interrante and co-workers have recently reinvestigated the reactions of Me₃Al and Et₃Al with NH₃, which lead to AlN.¹⁰ In our laboratory, the reaction chemistry of (Me₃Si)₃Al¹¹ with a variety of inorganic and organometallic reagents has been under examination, and it was reasoned that the weaker Si-Al bond, compared to the C-Al bond in aluminum alkyls, and the bulky steric environment in (Me₃Si)₃Al might provide a more useful aluminum precursor for the synthesis of AlN and other aluminum-bearing solid-state materials. We report here on reactions of (Me₃Si)₃Al-Et₂O with NH₃, the isolation and X-ray crystal structure determination for an intermediate molecular elimination-condensation product, [(Me₃Si)₂AlNH₂]₂ (1), and the pyrolysis chemistry of the dimer and a second polymeric species, which results in solid solutions of AlN and SiC.

Experimental Section

General Information. Standard inert-atmosphere techniques were used for the manipulations of all reagents and reaction products. Infrared spectra were recorded on a Nicolet 6000 FT-IR spectrometer from solution cells and KBr pellets. Mass spectra were recorded on a Finnegan mass spectrometer by using a heated solids probe. NMR spectra were obtained from Varian FT-80 and GE NT-360 spectrometers. All NMR samples were sealed in 5-mm tubes, and the spectra (¹³C, ¹H) were referenced with Me₄Si. Elemental analyses were performed by R. Ju of the UNM Analytical Services Laboratory and by Galbraith Laboratories.

Materials. Ammonia was obtained from Matheson Gas Products, and it was purified by trap to trap vacuum distillations and dried over sodium. (Me₃Si)₃Al-Et₂O was prepared as described in the literature.¹¹ All solvents were rigorously dried with appropriate drying agents and degassed. Solvent transfers were accomplished by vacuum distillation.

Reaction of (Me₃Si)₃Al-Et₂O and NH₃, 1:1 Ratio. (Me₃Si)₃Al-Et₂O (3.0 mmol, 0.96 g) was loaded into a 100-mL Schlenk vessel in a nitrogen-filled glovebag, and the flask was thoroughly evacuated. Ammonia (3.0 mmol) was measured manometrically on a calibrated vacuum system and condensed into the flask at -196 °C. The mixture was warmed slowly to room temperature, and a vigorous reaction occurred well below 0 °C accompanied by gas evolution. The mixture was then stirred for 48 h at 25 °C. Needlelike crystals deposited on the flask walls after about 15 h. Volatile byproducts were removed into a trap cooled to -196 °C, and 0.57 g of a colorless crystalline solid remained: 100% yield based upon formation of [(Me₃Si)₂AlNH₂]₂ (1); mp 82-83 °C. Anal. Calcd for Si₄Al₂N₂C₁₂H₄₀: Al, 14.25; Si, 29.66; C, 38.05; N, 7.40; H, 10.64. Found: Al, 14.84; Si, 27.23; C, 36.22; N, 6.78; H, 9.57. The accuracy of the elemental analyses was reduced by difficulties encountered in obtaining complete combustion of the samples. The compound is soluble in hydrocarbons, benzene, and Et₂O. Mass spectrum (70 eV) [*m/e* (assignment) relative intensity]: 378 (M⁺) 5, 363 (M - CH₃⁺) 20, 346 (M - C₂H₈⁺) 3, 305 (M - C₃H₉Si⁺) 100, 290 (M - C₄H₁₂Si⁺) 20, 288 (M - C₄H₁₄Si⁺) 23, 232 (M - C₆H₁₈Si₂⁺) 93, 189 (AlNSi₂C₆H₂₁⁺) 13,

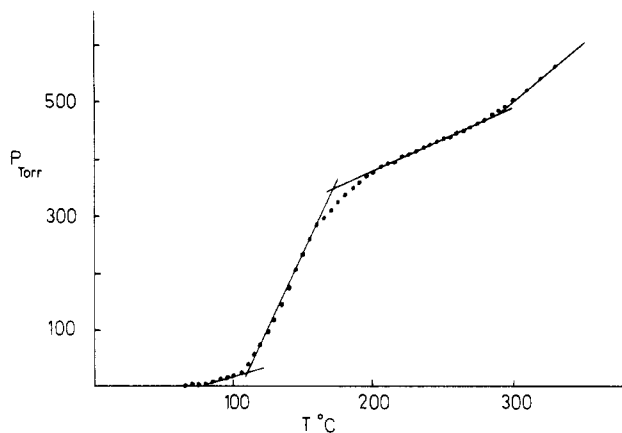


Figure 1. Thermolysis of [(Me₃Si)₂AlNH₂]₂ at 25-330 °C with total gas evolution as a function of temperature at a constant heating rate.

174 (AlNSi₂C₅H₁₇⁺) 12, 159 (AlNSi₂C₄H₁₄⁺) 6, 131 (AlN₂SiC₃H₁₂⁺) 18, 73 (SiC₃H₉⁺) 44. Infrared spectrum (cm⁻¹, C₆D₆): 3364 (m), 3313 (s), 2941 (s), 2887 (s), 1527 (m), 1466 (m), 1430 (m), 1386 (w), 1252 (m), 1238 (s), 904 (w), 828 (s), 730 (m), 679 (s), 642 (s), 608 (s), 553 (m). ¹³C{¹H} NMR (C₆D₆): δ 1.2 (Me₃Si). ¹H NMR (C₆D₆): δ 0.26 (Me₃Si, 18 H), 0.64 (NH, 2 H). The volatile byproducts were transferred to the vacuum system, and volumetric measurements showed a total of 5.9 mmol of gas collected. Infrared analysis of the gas mixture utilizing Beer's law calibration plots showed that the gas mixture contained equivalent amounts of Me₃SiH and Et₂O (3.0 mmol each).

Reaction of (Me₃Si)₃Al-Et₂O and Excess NH₃. (Me₃Si)₃Al-Et₂O (2.6 mmol, 0.84 g) was placed in a 100-mL Schlenk flask in a nitrogen-filled glovebag. Ammonia (7.8 mmol) was measured in the vacuum system and condensed into the flask at -196 °C. The mixture was warmed slowly to 25 °C, and a vigorous reaction occurred below 0 °C. After 5 days, the flask contained a small amount of a viscous oil and a white solid. The flask was maintained at 25 °C for a further 2 days, and then the volatiles were collected in the vacuum system. The white solid (2) was collected and found to be insoluble in hexane, benzene, and Et₂O. Reliable elemental analyses were not obtained due to incomplete combustion. The volatile products (10.4 mmol) were found to contain 2.4 mmol of NH₃, 5.4 mmol of Me₃SiH, and 2.6 mmol of Et₂O. Infrared spectrum of 2 (cm⁻¹, KBr): 3250 (s, br), 2915 (s), 2887 (m), 2110 (m), 1581 (sh), 1551 (m, br), 1513 (sh), 1248 (m), 905 (s, sh), 835 (s, br), 700 (s, br), 436 w, br).

Pyrolysis of [(Me₃Si)₂AlNH₂]₂ (1). [(Me₃Si)₂AlNH₂]₂ (1.5 mmol, 0.55 g) was placed in a Schlenk flask, and the flask was connected to a tensimeter.¹² The flask was then inserted into a small furnace and heated at a constant rate of 2 °C/min. Manometer pressure measurements were recorded every 5 °C between 25 and 330 °C. A typical profile is shown in Figure 1. At the conclusion of the thermolysis, the flask was cooled to 25 °C, and the volatile gases were collected and identified: Me₃SiH, 3.1 mmol; CH₄, 0.5 mmol. A white solid and a small amount of oil were retained in the flask.

In a companion pyrolysis scheme, 15.8 mmol (5.98 g) of [(Me₃Si)₂AlNH₂]₂ was placed in a 100-mL Schlenk flask, which was evacuated. The flask was then closed and heated at 300 °C for 24 h. After it had cooled to 25 °C, the volatiles were vacuum transferred into a -196 °C trap and subsequently determined (IR) to be Me₃SiH (40.7 mmol). The remaining glassy solid (2.96 g) displayed infrared absorptions (cm⁻¹, KBr) as follows: 3650 (w, br), 3250 (w, br), 2942 (m), 2883 (m), 2093 (w), 1343 (m), 850 (m, br). The solid was then ground into a fine powder, and 2.63 g of the powder was placed in a quartz tube. The tube was evacuated and heated to 600 °C for 24 h. The volatiles were recovered and identified: Me₃SiH, 1.1 mmol; CH₄, 30.8 mmol; H₂, 7.5 mmol. A white-gray solid (2.06 g) remained in the tube. An infrared spectrum (KBr) of the solid showed very weak, broad bands at ~3200, 2900, and 2100 cm⁻¹ and a very strong, broad absorption centered at 750 cm⁻¹. An X-ray powder pattern showed only very weak diffuse lines. The remaining solid was pyrolyzed under dynamic vacuum conditions at 930 °C for 86 h, and the off-gases were collected. The majority (90%) of the gas was evolved during the first 12 h: H₂, 2.0 mmol; CH₄, 0.6 mmol. The remaining solid (2.03 g) was characterized. Infrared spectrum (cm⁻¹, KBr): 1708 (w, br), 730 (vs, br). X-ray powder pattern (2θ, deg): 33.818, 36.091, 38.376, 50.111, 60.100, 71.369, 72.125.

- (5) Wynne, K. J.; Rice, R. W. *Annu. Rev. Mater. Sci.* **1984**, *14*, 297.
- (6) Kuramoto, N.; Taniguchi, H. *J. Mater. Sci. Lett.* **1984**, *3*, 471.
- (7) *Gmelin Handbuch der Anorganischen Chemie*; Verlag Chemie: Weinheim, BRD, 1934; Aluminum Teil B, p 132.
- (8) Chu, T. L.; Ing, D. W.; Noreika, A. *J. Solid-State Electron* **1967**, *10*, 1023.
- (9) Manasevit, H. M.; Erdman, F. M.; Simpson, W. I. *J. Electrochem. Soc.* **1971**, *118*, 1864. Morita, M.; Uesugi, N.; Isogai, S.; Tsubouchi, K.; Mikoshiba, N. *J. Appl. Phys., Jpn.* **1981**, *20*, 17. Rensch, U.; Eichorn, G. *Phys. Status Solidi A* **1983**, *77*, 195.
- (10) Interrante, L. V.; Carpenter, L. E.; Whitmarsh, C.; Lee, W.; Garbaskas, M.; Slack, G. A. *Mater. Res. Soc. Symp. Proc.* **1986**, *73*, 359. Hackney, M. J. L.; Interrante, L. V.; Whitmarsh, C. K.; Jiang, Z.; Slack, G. A. *Abstracts of Papers*, 193rd Meeting of the American Chemical Society, Denver, CO; American Chemical Society: Washington, DC, 1987; INORG 368. The structural parameters for [Me₂AlNH₂]₂ have not been published.
- (11) Röscher, L. *Angew. Chem., Int. Ed. Engl.* **1977**, *16*, 480. Röscher, L.; Altnau, G. *J. Organomet. Chem.* **1980**, *195*, 47.

- (12) Shriver, D. F. *The Manipulation of Air Sensitive Compounds*; McGraw-Hill: New York, 1969.

Table I. Summary of Crystal and Data Collection Parameters for [(Me₃Si)₂AlNH₂]₂

(A) Crystal Parameters at -25 (2) °C	
cryst syst: monoclinic	$M_r = 378.77$
space group: $P2_1/n$ (No. 14)	$V = 1277.4$ (4) Å ³
$a = 9.364$ (1) Å	$Z = 2$
$b = 8.171$ (2) Å	$F(000) = 416$
$c = 16.781$ (3) Å	$\rho_{\text{calcd}} = 0.98$ g cm ⁻³
$\beta = 95.78$ (1)°	$\mu(\text{Mo K}\alpha) = 2.93$ cm ⁻¹

(B) Data Collection Parameters	
radiation: Mo K α ($\lambda = 0.71069$ Å)	
monochromator: highly oriented graphite crystal	
scan speed: 4–30 min ⁻¹	
scan range: $[2\theta(\text{K}\alpha_1) - 1.1] - [2\theta(\text{K}\alpha_2) + 1.25]$ °	
2θ limits: $2 < \pm h, -k, +l < 55$ °	
bkgd counting time/total scan time: 0.5	
stds monitored: 3/141 reflctns [400, 040, 004];	
no signif changes in intens	
no. of reflctns colld: 4488	
no. of unique reflctns: 2940	
no. of unique data used: 2068, $F > 4.0\sigma(F)$	
no. of variables: 172	
GOF: 1.33	
R_F : 4.15%	
R_{wF} : 3.85%	
w : $1/[\sigma^2(F) + g F^2]$; $g = 0.00023$	

Pyrolysis of Polymeric Solid (2). A sample (0.21 g) of the polymeric solid (2) was placed in a quartz tube and heated in stages (300, 600, and 930 °C) as described above. The gases evolved were collected and identified (1.6 mmol of NH₃, 1.3 mmol of CH₄, and a very small amount of H₂). The remaining solid was partially characterized and found to give an IR spectrum comparable to that described above. The X-ray powder pattern shows reflections at the same 2θ values as listed above; however, the lines are much broader.

Crystal Structure Determination for [(Me₃Si)₂AlNH₂]₂. Single crystals were obtained as needles from a saturated hexane solution stored at 0 °C. A suitable crystal, 0.138 mm × 0.276 mm × 0.356 mm, was mounted under argon in a glass capillary and sealed. The crystal was centered on a P3/F automated diffractometer, and determinations of the crystal class, the orientation matrix, and accurate unit cell parameters were performed in a standard manner.¹³ The data were collected at -25 °C by the θ - 2θ technique using Mo K α radiation, a scintillation counter, and pulse height analyzer. Details of the data collection are summarized in Table I. Inspection of the data indicated the space group $P2_1/n$, and lattice constants were obtained from a least-squares fit to automatically centered settings for 25 reflections ($10.43 < 2\theta < 43.38$ °). A small empirical absorption correction based on ψ scans was applied to the data; the correction improved the azimuthal scan data agreement factor from 1.61% to 1.55%. The maximum and minimum transmissions were 0.162 and 0.135. The data were corrected for Lorentz and polarization effects, the redundant data averaged, and the space group extinct reflections removed. No signs of crystal decay were observed.

Solution and Refinement of the Structure. All calculations were performed on a SHELXTL structure determination system.¹⁴ Neutral-atom scattering factors and anomalous dispersion factors were used for all non-hydrogen atoms during the refinements. The scattering factors were taken from the analytical expressions given in ref 14. Both real ($\Delta f'$) and imaginary ($\Delta f''$) components of the anomalous dispersion were included. The function¹⁵ minimized during the least-squares refinements was $\sum w(|F_o| - |F_c|)^2$.

The solution and refinement of the structure were based on 2940 unique, space group allowed reflections, of which 2068 reflections were considered above the $4.0\sigma(F)$ level. The structure was solved by direct methods. The best E map gave trial positions for Al and two Si atoms.

Table II. Non-Hydrogen Positional Parameters and Their Esd's for [(Me₃Si)₂AlNH₂]₂

atom	x/a	y/b	z/c
Al(1)	0.118 19 (7)	0.608 76 (8)	0.500 45 (4)
Si(1)	0.162 01 (7)	0.819 35 (8)	0.606 32 (4)
C(1)	0.297 98 (34)	0.972 64 (36)	0.579 90 (19)
C(2)	-0.002 29 (30)	0.939 45 (39)	0.624 95 (17)
C(3)	0.232 44 (39)	0.729 52 (42)	0.705 72 (18)
Si(2)	0.268 42 (8)	0.576 38 (9)	0.388 89 (4)
C(4)	0.396 50 (46)	0.749 58 (58)	0.380 91 (23)
C(5)	0.152 40 (43)	0.570 23 (70)	0.291 83 (21)
C(6)	0.376 62 (44)	0.382 44 (61)	0.397 75 (25)
N(1)	0.082 51 (23)	0.393 59 (26)	0.545 13 (14)

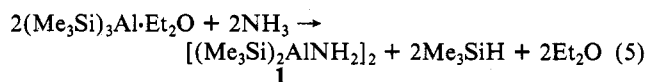
Table III. Bond Distances (Å) and Their Esd's for [(Me₃Si)₂AlNH₂]₂

Al(1)–Si(1)	2.478 (1)	Al(1)–Si(2)	2.467 (1)
Al(1)–N(1)	1.953 (2)	Al(1)–Al(1')	2.838 (1)
Al(1)–N(1')	1.956 (2)	Si(1)–C(1)	1.871 (3)
Si(1)–C(2)	1.877 (3)	Si(1)–C(3)	1.880 (3)
Si(2)–C(4)	1.869 (5)	Si(2)–C(5)	1.865 (4)
Si(2)–C(6)	1.879 (5)	N(1)–Al(1')	1.956 (2)

A structure factor calculation and difference map gave trial positions for the rest of the non-hydrogen atoms. Refinement of the positional and individual isotropic thermal parameters on the non-hydrogen atoms gave convergence at $R_F = 11.4\%$ and $R_{wF} = 13.3\%$. Individual anisotropic thermal parameters were applied, and refinement gave $R_F = 6.4\%$ and $R_{wF} = 7.0\%$. In the final cycles, the hydrogen atoms were allowed to vary in position, but their U_{iso} 's were fixed equal to 1.2 times the last U_{equiv} of their parent atom. A final least-squares refinement gave $R_F = 4.2\%$ and $R_{wF} = 3.9\%$ for 153 variables and 2068 reflections. A final difference Fourier synthesis showed no unusual features with no peak greater than $0.25 \text{ e } \text{Å}^{-3}$. Tables of observed and calculated structure factors, anisotropic thermal parameters, and hydrogen atom positional parameters are available in the supplementary material. Non-hydrogen positional parameters are summarized in Table II.

Results and Discussion

Combination of (Me₃Si)₃Al·Et₂O and NH₃ in a 1:1 ratio without solvent resulted in a vigorous reaction at a temperature well below 0 °C, and the outcome of the reaction is summarized in eq 5. The volatile byproducts were quantitatively recovered



in a calibrated vacuum system and identified by infrared spectroscopy. The previously unknown elimination–condensation product, [(Me₃Si)₂AlNH₂]₂ (1), was isolated in quantitative yield as colorless needles following removal of the volatile byproducts. Unlike the case of parallel system, Me₃Al and NH₃, where the simple addition compound Me₃Al·NH₃ may be isolated,^{10,16} no evidence for a stable adduct, (Me₃Si)₃Al·NH₃, was found under the conditions examined. The crystals were not pyrophoric; however, they decomposed over 1 h in moist air, as evidenced by the formation of a milky coat on the surface of the crystals. The compound was indefinitely stable under dry nitrogen at 25 °C, and it decomposed only slightly over 24 h in boiling toluene.

Compound 1 was characterized by elemental analysis and mass, infrared, and NMR spectroscopy. The mass spectrum showed a parent ion at m/e 378 and several fragment ions consistent with the proposed dimeric formulation. The infrared spectrum, obtained in C₆D₆ solution, gave two sharp, medium-intensity bands in the ν_{NH} region at 3364 and 3313 cm⁻¹, a strong and medium-intensity pair of sharp bands in the ν_{CH} region at 2941 and 2887 cm⁻¹, and a series of strong- to medium-intensity bands in the region 1252–553 cm⁻¹. The ¹H NMR spectrum of 1 showed two resonances, δ 0.26 and 0.64 (broad) of area ratio ~9:1, that are assigned to the (H₃C)₃Si and H₂N protons, respectively. The shift

(13) Programs used for centering reflections, autoindexing, refinement of cell parameters, and axial photographs are those described in: "Nicolet P3/R3 Operations Manual"; Sparks, R. A., Ed.; Syntex Analytical Instruments: Cupertino, CA, 1978.

(14) The SHELXTL package of programs for calculations and plots is described in: Sheldrick, G. M. "SHELXTL Users Manual, Revision 3"; Nicolet XRD Corp.: Cupertino, CA, 1981. SHELXTL uses scattering factors and anomalous dispersion terms taken from: *International Tables for X-ray Crystallography*; Kynoch: Birmingham, England, 1968; Vol. IV.

(15) Discrepancy indices are defined as follows: $R_F = [\sum |F_o| - |F_c|] / \sum |F_o|$, $R_{wF} = [\sum w|F_o| - |F_c|]^2 / \sum w|F_o|^2]^{1/2}$, and the goodness of fit GOF = $[\sum (|F_o| - |F_c|)^2 / (\text{NO} - \text{NV})]^{1/2}$, where NO is the number of observations and NV is the number of variables.

(16) Studies by E. Wiberg discussed by: Bahr, G. *FIAT Review of German Science 1939–1946*; Dieterichsche Verlagsbuchhandlung: Wiesbaden, BRD, 1948; Inorganic Chemistry, Part II. Ziegler, K.; Gillbert, H. *Justus Liebigs Ann. Chem.* 1960, 629, 20.

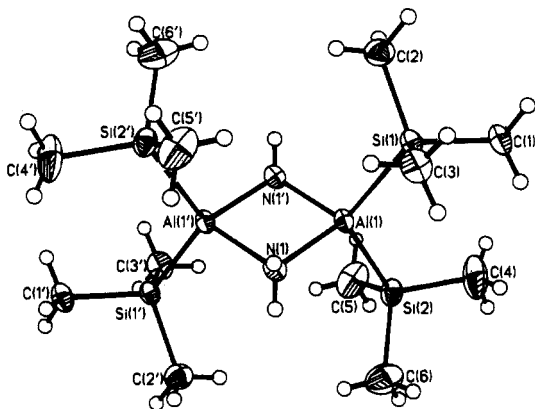


Figure 2. Molecular structure and atom-labeling scheme for $[(\text{Me}_3\text{Si})_2\text{AlNH}_2]_2$ (50% thermal ellipsoids).

Table IV. Bond Angles (deg) and Their Esd's for $[(\text{Me}_3\text{Si})_2\text{AlNH}_2]_2^a$

Si(1)–Al(1)–Si(2)	123.6	Si(1)–Al(1)–N(1)	111.8 (1)
Si(2)–Al(1)–N(1)	109.1 (1)	Si(1)–Al(1)–Al(1')	120.8 (1)
Si(2)–Al(1)–Al(1')	115.7	N(1)–Al(1)–Al(1')	43.5 (1)
Si(1)–Al(1)–N(1')	111.7 (1)	Si(2)–Al(1)–N(1')	107.5 (1)
N(1)–Al(1)–N(1')	86.9 (1)	Al(1')–Al(1)–N(1')	43.4 (1)
Al(1)–Si(1)–C(1)	111.2 (1)	Al(1)–Si(1)–C(2)	113.8 (1)
C(1)–Si(1)–C(2)	106.2 (1)	Al(1)–Si(1)–C(3)	112.5 (1)
C(1)–Si(1)–C(3)	106.6 (1)	C(2)–Si(1)–C(3)	106.0 (1)
Al(1)–Si(2)–C(4)	113.1 (1)	Al(1)–Si(2)–C(5)	109.8 (1)
C(4)–Si(2)–C(5)	106.2 (2)	Al(1)–Si(2)–C(6)	112.0 (1)
C(4)–Si(2)–C(6)	107.4 (2)	C(5)–Si(2)–C(6)	108.0 (2)
Al(1)–N(1)–Al(1')	93.1 (1)		

^aThe primed atoms are obtained from the unprimed-atom coordinates with the following transformation: $-x, 1-y, 1-z$.

for the amino protons falls within the normal range experienced with aminoalanes.¹⁷ The $^{13}\text{C}\{^1\text{H}\}$ NMR spectrum showed a single resonance, δ 1.21, indicative of a single trimethylsilyl environment.

The above data offer sound characterization of **1**; however, identification of the degree of association of the monomer unit $(\text{Me}_3\text{Si})_2\text{AlNH}_2$ is not certain. It is appropriate to note that in the parallel chemical system, $[\text{Me}_2\text{AlNH}_2]_n$, Wiberg¹⁶ utilized gas-phase molecular weight measurements to deduce a dimeric formulation. Recent single-crystal X-ray diffraction analysis, on the other hand, revealed that this compound is trimeric in the solid state with a puckered cyclohexane-like ring structure.¹⁰ In order to unambiguously determine the degree of association of **1**, the molecular structure was determined by single-crystal X-ray diffraction analysis, and the results are described here. A view of the molecule is shown in Figure 2, and interatomic distances and angles are summarized in Tables III and IV.

The X-ray crystal structure determination of **1** reveals that the molecule is dimeric with crystallographic C_2 symmetry. The structure contains a planar Al_2N_2 ring with two eclipsed Me_3Si groups on each aluminum atom and two hydrogen atoms on each nitrogen atom. The planar Al_2N_2 ring is nearly square with structural parameters $\text{Al}(1)\text{--N}(1) = 1.953(2) \text{ \AA}$, $\text{Al}(1)\text{--N}(1') = 1.956(2) \text{ \AA}$, $\text{N}(1)\text{--Al}(1)\text{--N}(1') = 86.9(1)^\circ$, and $\text{Al}(1)\text{--N}(1)\text{--Al}(1') = 93.1(1)^\circ$. The planar, dimeric structure is similar to the structure of $[\text{Me}_2\text{AlNMe}_2]_2$, $\text{Al}\text{--N} = 1.958(5) \text{ \AA}$,^{18,19} while the structure determinations for $[\text{Me}_2\text{AlNH}_2]_3$ ¹⁰ and $[\text{H}_2\text{AlNMe}_2]_3$, $\text{Al}\text{--N} = 1.93(3) \text{ \AA}$,²⁰ reveal trimeric structures. The $\text{Al}\text{--N}$ bond distances in **1** fall in a range, 1.91–1.97 \AA , found in a number of dimeric and trimeric organoaluminum amides.

Although other factors may play a role, it is likely that the large steric effects imposed by the bulky Me_3Si groups are responsible for the appearance of the dimeric structure for **1**.

The average $\text{Al}\text{--Si}$ distance in **1**, 2.472 \AA , is identical with the distances reported for $(\text{Me}_3\text{Si})_3\text{Al}\cdot\text{OEt}_2$, 2.47 \AA ,²¹ and $(\text{Me}_3\text{Si})_3\text{Al}\cdot\text{TMEDA}$, 2.472 (3) \AA .²² The $\text{Al}\text{--Si}$ distances, as noted by Oliver,²² are slightly greater than the sum of the covalent radii, 2.43 \AA . The average $\text{Si}\text{--C}$ bond distance in **1**, 1.874 \AA , is also comparable with those found in the two $(\text{Me}_3\text{Si})_3\text{Al}$ complexes. As expected for a ring system, the $\text{Si}\text{--Al}\text{--Si}$ bond angle in **1**, 123.6 (1)°, is significantly greater than the average angle in $(\text{Me}_3\text{Si})_3\text{Al}\cdot\text{TMEDA}$, 111.2°, and the average $\text{Si}\text{--Al}\text{--N}$ bond angle in **1**, 110.0°, is slightly larger than the average $\text{Si}\text{--Al}\text{--N}$ angle in $(\text{Me}_3\text{Si})_3\text{Al}\cdot\text{TMEDA}$. The $\text{Al}(1)\text{--Al}(1')$ separation in **1**, 2.838 (1) \AA , is longer than the $\text{Al}\text{--Al}$ separation in $[\text{Me}_2\text{AlNMe}_2]_2$, 2.809 (4) \AA , consistent with the slightly more acute $\text{N}\text{--Al}\text{--N}$ internal ring angle in **1**.

Combination of $(\text{Me}_3\text{Si})_3\text{Al}\cdot\text{OEt}_2$ and NH_3 in a 1:3 ratio, with the entire quantity of NH_3 added at one time, after 5–7 days at 25 °C, resulted in the formation of a white powdery solid (**2**).²³ Analysis of the volatiles showed consumption of only 2 equiv of NH_3 and evolution of 1 equiv of Et_2O and 2 equiv of Me_3SiH . The solid was insoluble in hexane, benzene, and Et_2O , and it slowly decomposed in air with evolution of NH_3 . Attempts, to date, to obtain reliable elemental analyses have been frustrated by incomplete combustion. In addition, attempts to obtain a mass spectrum by thermal evaporation of a sample into the ionization chamber have led to only low-mass ions characteristic of decomposition fragments. The infrared spectrum of **2** is distinctly different from the spectrum of **1**. A single, very broad absorption, centered at 3250 cm^{-1} , replaces the two sharp $\text{N}\text{--H}$ stretching absorptions of **1**. In addition, the numerous sharp intense absorptions for **1** in the region 1600–600 cm^{-1} are replaced by broad absorptions at 1551, 1248, 905, 835, and 700 cm^{-1} . These properties suggest that **2** is a polymeric solid, and on the basis of the byproduct gas analysis, a formulation, $[(\text{Me}_3\text{Si})\text{Al}(\text{NH}_2)_2]_n$, is tentatively proposed.

The thermal decomposition chemistry of **1** and **2** was of interest in the context of comparisons of stabilities of alkylaluminum- and silylaluminum-Lewis base complexes, as well as the screening of these compounds as potential aluminum nitride precursors. It is important to note again that, unlike the case of $\text{Me}_3\text{Al}\cdot\text{NH}_3$,^{2-4,10,16,24} which is stable at 25 °C, there is no indication of the formation of a stable adduct, $(\text{Me}_3\text{Si})_3\text{Al}\cdot\text{NH}_3$. Instead, facile elimination chemistry proceeds between the acid and base fragments well below 0 °C. The thermolysis of **1** at a constant heating rate (5 °C/min) was first examined in a tensimeter²⁵ between 25 and 330 °C. A plot of gas pressure vs temperature is shown in Figure 1. Between 25 and 80 °C, no pressure was registered, and the compound melted at 82 °C. From 85 to 105 °C, a small, linear PV/nR behavior was noted. From 105 to ~170 °C, a rapid increase in pressure with increasing temperature was observed, and subsequent analysis of the gas phase showed formation of Me_3SiH (2 equiv/dimer unit of **1**). Between ~200 and 275 °C, there was a second region of linear PV/nR behavior paralleling the behavior in the range 85–105 °C. Above 300 °C, a second gas evolution stage began that produced methane. This heating profile guided the further pyrolysis studies of **1** and **2**.

The pyrolysis of **1** was then followed in stages. For example, 5.98 g (15.8 mmol) of **1** was heated for 24 h in an evacuated tube at 300 °C. Trimethylsilane (40.7 mmol, 2.6 equiv) was collected

(17) Amirghalili, S.; Hitchcock, P. B.; Jenkins, A. D.; Nyathi, J. Z.; Smith, J. D. *J. Chem. Soc., Dalton Trans.* **1981**, 377.

(18) McLaughlin, G. M.; Sim, G. A.; Smith, J. D. *J. Chem. Soc., Dalton Trans.* **1972**, 2197.

(19) Von Hess, H.; Hinderer, A.; Steinhäuser, S. Z. *Anorg. Allg. Chem.* **1970**, 377, 1.

(20) Semenenko, K. N.; Lobkovskii, E. B.; Dorosinskii, A. L. *Zh. Strukt. Khim.* **1972**, 13, 743.

(21) Rösch, L.; Altnau, G.; Erb, W.; Pickardt, J.; Bruncks, N. *J. Organomet. Chem.* **1980**, 197, 51.

(22) Geobel, D. W.; Hencker, J. L.; Oliver, J. P. *Organometallics* **1983**, 2, 746.

(23) An intermediate product may be isolated from reactions of NH_3 and $(\text{Me}_3\text{Si})_3\text{Al}\cdot\text{Et}_2\text{O}$ in reactant ratios of 2 or greater, and the nature of this product is under examination.

(24) Laubengayer, A. W.; Smith, J. D.; Ehrlich, G. G. *J. Am. Chem. Soc.* **1961**, 83, 542.

(25) This technique was utilized, in part, because of our present inability to obtain classical thermal analysis (TGA, DTA) without brief exposure of the reactive samples to air.

along with 2.96 g of an easily handled white glassy solid. Attempts to obtain an elemental analysis of the solid material were unsuccessful due to incomplete combustion of the material. An X-ray powder pattern showed that this material is amorphous. An infrared spectrum of the solid showed a very weak, broad absorption at $\sim 3220\text{ cm}^{-1}$, assigned to N-H stretches, a sharp doublet at 2942 and 2883 cm^{-1} , assigned to C-H stretches, a medium-intensity, broad absorption at $\sim 2100\text{ cm}^{-1}$, assigned to Si-H stretches, a broad band at 1343 cm^{-1} , and a very broad absorption centered at $\sim 800\text{ cm}^{-1}$. The Si-H vibration is presumed to result from thermal cleavage of Si-CH₃ groups and subsequent formation of Si-H bonds. Such processes and spectral features have been observed during the production of polycarbosilanes and silicon carbide.²⁶

A sample (2.63 g) of the glassy solid was then heated in a quartz tube for 24 h at 600 °C. The volatiles were collected and identified: H₂, 7.5 mmol; CH₄, 30.8 mmol; Me₃SiH, 1.1 mmol. The solid product (2.06 g) was light gray. It showed very weak, broad infrared absorptions at ~ 3200 , 2900, and 2100 cm^{-1} , and a very strong, broad absorption centered at $\sim 750\text{ cm}^{-1}$. The last band is very typical of authentic samples of AlN.²⁷ An X-ray powder pattern of the solid showed only weak, diffuse lines.

This solid was then heated at 930 °C for 86 h. Small amounts of H₂ and CH₄ were evolved, and 2.03 g of a light gray solid was recovered. The infrared spectrum showed only a very strong absorption at $\sim 730\text{ cm}^{-1}$; however, the powder pattern showed relatively sharp lines characteristic of AlN.^{28,29} Subsequent energy-dispersive X-ray analysis also showed the presence of Si.³⁰ The last observation, the incomplete loss of Me₃SiH, the appearance of CH₄ in the volatile byproducts during heating above 300 °C, and the well-documented formation of SiC from carbosilane polymers^{26,31} suggest that the AlN prepared from 1 contains SiC. In fact, SiC and AlN are known to have the same wurtzite

crystal structure with nearly identical lattice constants: SiC, $a = 3.07\text{ \AA}$, $c = 5.04\text{ \AA}$; AlN, $a = 3.11\text{ \AA}$, $c = 4.98\text{ \AA}$. They are also known to form solid solutions in all proportions. The estimated lattice constants from the powder patterns obtained here are $a = 3.08\text{ \AA}$ and $c = 4.97\text{ \AA}$. Unfortunately, the infrared spectra offer little help in identifying SiC in AlN since the spectra of the pure phases are nearly identical.

The thermolysis of the polymeric solid 2 was also examined in stages. Heating the solid from 25 to 600 °C over 48 h led to evolution of NH₃ and CH₄ (~ 1 equiv each) and small amounts of H₂. After this stage, the solid product was heated to 930 °C for 90 h, and an additional small amount of CH₄ was evolved. The resulting light gray solid had an IR spectrum identical with that of the final thermolysis product obtained from 1. The X-ray powder pattern for this material showed reflections in the expected region; however, they were considerably broader than those observed for the powder described above. The incomplete loss of Me₃SiH and CH₄ suggests that carbon may be retained in this material.³²

On the basis of these studies, the elimination-condensation reaction chemistry of (Me₃Si)₃Al with NH₃ is found to be more facile than that found for Me₃Al and NH₃. 1 and 2 are useful precursors for the formation of solid solutions of AlN and SiC. In fact, there appears to be some useful benefit to the inclusion of SiC in this molecular synthetic approach, and the characterization of the sintering process of these materials is in progress. Additional studies of the synthesis and characterization of the ceramic products are in progress in collaboration with investigators at Sandia National Laboratories.

Acknowledgment. R.T.P. wishes to recognize the support of the National Science Foundation (Grant CHE-8503550) for support of this research. We also acknowledge support from the National Science Foundation that facilitated the purchase of the high-field NMR spectrometer (Grant CHE-8201374).

Registry No. 1, 111290-98-3; 2, 111290-99-4; (Me₃Si)₃Al, 65343-66-0; NH₃, 7664-41-7; aluminum silicon carbide nitride, 111409-04-2.

Supplementary Material Available: Tables SI and SII, listing thermal parameters and hydrogen atom positional parameters (2 pages); Table SII, listing calculated and observed structure factors (10 pages). Ordering information is given on any current masthead page.

- (26) Yajima, S.; Hasegawa, Y.; Hayashi, J.; Iimura, M. *J. Mater. Sci.* **1978**, *13*, 2569. Yajima, S.; Omori, M.; Hayashi, J.; Okamura, K.; Matsuzawa, T.; Liaw, C. F. *Chem. Lett.* **1976**, 551. Hasegawa, Y.; Iimura, M.; Yajima, S. *J. Mater. Sci.* **1980**, *15*, 720.
 (27) Brame, E. G.; Margrave, J. L.; Maloch, V. M. *J. Inorg. Nucl. Chem.* **1957**, *5*, 48.
 (28) Taylor, K. M.; Lenie, C. *J. Electrochem. Soc.* **1960**, *107*, 308.
 (29) X-ray powder pattern indexing 2θ , deg (hkl): 33.818 (100), 36.091 (002), 38.376 (101), 50.111 (102), 60.100 (110), 71.369 (200), 72.125 (112).
 (30) Quantitative energy-dispersive X-ray analysis for Al, Si, and the light-Z elements will be undertaken shortly. The present semiquantitative analysis for Al and Si indicates an approximately 2:1 ratio.
 (31) West, R. *J. Organomet. Chem.* **1986**, *300*, 327.

- (32) AlN is known to incorporate carbon, leading to carbonitrides: Jeffrey, G. A.; Wu, V. Y. *Acta Crystallogr.* **1963**, *16*, 554. *Ibid.* **1966**, *20*, 538. Takahashi, Y.; Mutoh, K.; Motojima, S.; Sugiyama, K. *J. Amer. Chem. Soc.* **1981**, *103*, 1217. Takahashi, Y.; Yamashita, K.; Motojima, S.; Sugiyama, K. *Surf. Sci.* **1979**, *86*, 238.